

# Energy accommodation coefficient extracted from acoustic resonator experiments

Felix Sharipov<sup>a)</sup> and Michael R. Moldover<sup>b)</sup>

National Institute of Standards and Technology, 100 Bureau Drive, Gaithersburg, Maryland 20899

(Received 28 July 2016; accepted 17 October 2016; published 2 November 2016)

The authors review values of the temperature jump coefficient  $\zeta_T$  determined from measurements of the acoustic resonance frequencies  $f_{\text{acoust}}$  of helium-filled and argon-filled, spherical cavities near ambient temperature. The authors combine these values of  $\zeta_T$  with literature data for tangential momentum accommodation coefficient (TMAC) and the Cercignani-Lampis model of the gas–surface interaction to obtain measurement-derived values of the normal energy accommodation coefficient (NEAC). The authors found that NEAC ranges from 0 to 0.1 for helium and from 0.61 to 0.85 for argon at ambient temperature for several different surfaces. The authors suggest that measurements of  $f_{\text{acoust}}$  of gas-filled, cylindrical cavities and of the nonradial modes of quasispherical cavities might separately determine TMAC and NEAC. Alternatively, TMAC and NEAC could be determined by measuring the heat transfer and momentum transfer between parallel rotating disks at low pressure.

© 2016 American Vacuum Society. [<http://dx.doi.org/10.1116/1.4966620>]

## I. INTRODUCTION

Accommodation coefficients (ACs) play an important role in description of rarefied gas flows.<sup>1–3</sup> They represent particular integrals of the gas–surface interactions allowing us to avoid a detailed descriptions of these complex interactions and, at the same time, to predict more precisely the behavior of gases in vacuum systems, microfluidics, around space vehicles, and in other situations when rarefied gas flows encounter solid surfaces. Usually, ACs are not measured directly; instead, they are extracted from experiments using specific models for the gas–solid interactions, such as the simple diffuse-specular scattering or the Cercignani-Lampis (CL) model.<sup>4</sup> The latter will be used here. If ACs determined in one experiment are used to describe another experiment, both experiments must have similar solid surfaces, both must use the same gas, and both must be interpreted using the same model for the gas–solid interactions.

Today, there is extensive literature providing values of the tangential momentum accommodation coefficient (TMAC) extracted from diverse experiments.<sup>5–7</sup> However, reliable values of the normal energy accommodation coefficient (NEAC) are rare because of the difficulty in measuring the quantities used to extract NEAC. In the present work, we extract the NEAC from the literature of measurements of the acoustic resonance frequencies of gas-filled, quasispherical, metal-walled cavities. These well-documented measurements were performed to determine the Boltzmann constant and the thermodynamic temperature with small uncertainties using different kinds of acoustic resonators.<sup>8–24</sup> To attain low uncertainties, the temperature jump at the gas–surface interface is taken into account by using the model for radially symmetric, acoustic standing waves in the cavity. Moreover, the NEAC is extracted from experimental data on heat transfer.<sup>25,26</sup> In general, the temperature jump and heat

transfer are determined by both the TMAC and NEAC so that the diffuse-specular model containing only one parameter is not appropriate for our purpose; instead, the CL model<sup>4</sup> providing more complete description of the gas–solid interaction will be used here.

The paper is organized as follows: Accommodation coefficients are defined in Sec. II. The temperature jump coefficient and its application to acoustic resonance are described in Sec. III. The values of ACs extracted from various experiments are given in Sec. IV. Discussions and recommendations of new experiments to measure the ACs are presented in Sec. V.

## II. DEFINITION OF ACCOMMODATION COEFFICIENTS

The AC of some property  $\psi$  is defined as<sup>1–3</sup>

$$\alpha(\psi) = \frac{J(\psi)}{J_{\text{diff}}(\psi)}, \quad J(\psi) = \int v_n \psi(\mathbf{v}) f(\mathbf{v}) d\mathbf{v}, \quad (1)$$

where  $\mathbf{v}$  is the molecular velocity,  $v_n$  is its component normal to a surface element where the AC is calculated,  $f$  is the velocity distribution function,  $J$  is the actual flux of the property  $\psi$  normal to the surface, and  $J_{\text{diff}}$  is the same flux assuming the complete accommodation (diffuse scattering) of gaseous particles on the surface. For example, if we assume  $\psi = mv$ , where  $m$  is the particle mass and  $v_t$  is its tangential velocity, then  $\alpha$  will be the TMAC denoted as  $\alpha_t$ . In another example, if  $\psi = mv^2/2$  then  $\alpha$  is the AC of the total kinetic energy. It is common to consider only the part of the kinetic energy corresponding to the normal molecular velocity, i.e.,  $\psi = mv_n^2/2$ . The coefficient corresponding to this property is the NEAC further denoted as  $\alpha_n$ . The use of the ACs simplifies interpretations of experimental data, but some issues pointed out below should be considered in such interpretations.

The diffuse-specular scattering model assumes that a fraction  $h$  of incident particles is scattered diffusely, while the

<sup>a)</sup>Present address: Departamento de Física, Universidade Federal do Paraná, Curitiba 81531-980, Brazil; electronic mail: sharipov@fisica.ufpr.br

<sup>b)</sup>Electronic mail: michael.moldover@nist.gov

remaining fraction  $(1-h)$  is reflected specularly. If we employ this model to calculate the accommodation coefficient  $\alpha$  based on Eq. (1), it will be equal to the fraction  $h$  for any property  $\psi$  and for any incident distribution function. However, the values of  $\alpha_t$  extracted from various experiments on gas flows<sup>5-7</sup> are quite different from the values of  $\alpha_n$  extracted from experiments on heat transfer.<sup>25,27</sup> Moreover, the diffuse-specular model is inconsistent with experimental data on the thermomolecular pressure difference.<sup>28,29</sup>

In contrast to this model, the CL gas-surface interaction kernel<sup>4</sup> contains two independent parameters  $\alpha_t$  and  $\alpha_n$ . This model is consistent with measurements of the thermomolecular pressure differences. The CL kernel was constructed so that the TMAC  $\alpha_t$  and NEAC  $\alpha_n$  calculated by Eq. (1) on the basis of the CL model do not vary for different distribution functions of incident particles so that it is expected that their values will be not sensitive to the type of gas flow. Thus, the CL model is a more versatile description of the gas-surface interactions than the widely used diffuse-specular law.

In the free-molecular regime, some quantities can be expressed analytically in terms of the ACs by applying the CL model. For instance, in the case of heat transfer through a gas confined between two parallel plates having a small temperature difference  $\Delta T$ , the heat flux reads<sup>30</sup>

$$q = \frac{pv_m\Delta T}{2\sqrt{\pi}T} \left[ \frac{\alpha_n}{2-\alpha_n} + \frac{\alpha_t(2-\alpha_t)}{2-\alpha_t(2-\alpha_t)} \right], \quad (2)$$

where  $p$  is the gas pressure,  $T$  is the average temperature of the plates,  $v_m$  is the most probable speed of gaseous particles given by

$$v_m = \sqrt{2k_B T/m}, \quad (3)$$

and  $k_B$  is the Boltzmann constant.

### III. TEMPERATURE JUMP AND ACOUSTIC RESONANCE

As is well known, in a nonequilibrium state, the gas temperature  $T_g$  near a surface is not equal to the surface temperature  $T_s$ ; instead, there is a temperature jump which is proportional to the normal temperature gradient in the gas. Let  $x$  be a coordinate normal to a flat surface with the origin at the surface and directed toward the gas. Then, the temperature jump can be written as<sup>2,3</sup>

$$T_g - T_s = \zeta_T \ell \frac{dT_g}{dx} \quad \text{at } x = 0, \quad (4)$$

where  $\zeta_T$  is the temperature jump coefficient,  $\ell$  is the equivalent free path defined as

$$\ell = \frac{\mu v_m}{p}, \quad (5)$$

$p$  is the local pressure of the gas,  $\mu$  is the gas viscosity, and  $v_m$  is calculated by Eq. (3) using the surface temperature  $T_s$ .

Considering the Fourier law, Eq. (4) can be also written in term of the normal heat flux  $q_x$

$$T_g - T_s = -\zeta_T \ell \frac{q_x}{\kappa}, \quad q_x = -\kappa \frac{dT_g}{dx}, \quad (6)$$

where  $\kappa$  is the heat conductivity of the gas. Note that the jump condition (4) or (6) is applied to any surface with a curvature radius  $R_c$  significantly larger than the equivalent free path,  $R_c \gg \ell$ . Under this condition, the curvature is negligible, and the surface can be considered flat.

During last decades, the temperature jump coefficient was calculated by many researchers starting with the kinetic Boltzmann equation.<sup>5,31-34</sup> An extensive list of the corresponding publications and critical analysis of numerical data on the jump coefficient can be found in the review.<sup>7</sup> Application of the temperature jump condition, Eqs. (4) or (6), allows us to obtain analytical solutions of some classical problems of heat transfer. For instance, the radial heat transfer  $q_r$  between two coaxial cylinder having a small temperature difference  $\Delta T$  is given by<sup>7</sup>

$$q_r = \kappa \frac{\Delta T}{r} \left[ \ln \frac{b}{a} + \frac{\zeta_T}{\delta} \left( 1 + \frac{a}{b} \right) \right]^{-1}, \quad (7)$$

where  $\kappa$  is the gas heat conductivity,  $a$  and  $b$  are inner and outer cylinder radii, respectively, and  $\delta$  is the gas rarefaction parameter

$$\delta = pa/(\mu v_m). \quad (8)$$

Note that expression (7) is valid for large values of the rarefaction parameter  $\delta \gg 1$ .

Another form of the temperature jump is used in the papers,<sup>9,10,15-17,21,22</sup> namely,

$$T_g - T_s = -l_a \frac{q_x}{\kappa}, \quad (9)$$

where  $l_a$  is the thermal accommodation length defined as

$$l_a = \frac{\kappa}{p} \left( \frac{\pi m T_s}{2k_B} \right)^{1/2} \frac{1}{c_V/k_B + 1/2} \frac{2-h}{h}, \quad (10)$$

and  $c_V$  is the specific heat per particle at constant volume. The definition given by Eqs. (9) and (10) is based on the Maxwell theory of the velocity slip and temperature jump phenomena.<sup>35</sup> The main assumption of this theory is that the stream of molecules approaching to a solid surface is the same as it is in the midst of the gas. In other words, the velocity distribution function in the Knudsen layer is not obtained; instead, its approximate expression is used to calculate macroscopic quantities. Moreover, the diffuse-specular gas-surface interaction model was applied to obtain Eq. (10) assuming  $h$  to be the fraction of diffusely scattered particles. Despite this quantity is frequently referred as thermal AC, the scattering model applied to derive (10) does not relate  $h$  to some specific molecular property  $\psi$ .

Ewing *et al.*<sup>9</sup> calculated the effects of the temperature jump on the frequencies of the radially symmetric acoustic modes of gas-filled spherical cavities surrounded by metal

walls. For these modes, the acoustic velocity is perpendicular to the solid walls. As the gas acoustic pressure oscillates, the gas temperature oscillates too. During each acoustic cycle, heat is exchanged between the gas and the solid within thermal boundary layers at the gas–solid interface. Ewing *et al.*<sup>9</sup> concluded that a temperature jump at the gas–solid boundary increases the resonance frequencies and leaves the half-widths of the resonances unchanged. For a low-density, monatomic gas, the frequency  $f_i$  of the  $i$ th radially symmetric acoustic mode increases by  $\Delta f_i$  according to

$$\frac{\Delta f_i}{f_i} = \frac{(\gamma - 1)l_a}{a} \equiv \frac{A_{-1}p^{-1}}{2u_0^2}, \quad (11)$$

where  $a$  is the radius of the spherical cavity,  $\gamma = c_p/c_V = 5/3$  is the heat-capacity ratio,  $p$  is the pressure,  $u_0$  is the speed of sound in the limit  $p \rightarrow 0$ , and  $A_{-1}$  is a parameter that is fitted to  $f_i(p)$ . Several groups (Table I) measured the pressure dependence of the acoustic resonance frequencies  $f_i(p)$  and corrected the data for well-understood perturbations.<sup>9,10,20</sup> Then, they determined  $A_{-1}$  and  $l_a$  in Eq. (11).

A combination of Eqs. (6), (9), and (10) leads to the following relation of the temperature jump coefficient to  $h$ :

$$\zeta_T = \frac{5\sqrt{\pi}}{4Pr} \frac{1}{c_V/k_B + 1/2} \frac{2-h}{h}, \quad (12)$$

where  $Pr$  is the Prandtl number determined by viscosity  $\mu$  and heat conductivity  $\kappa$ . Using the numerical values of  $\mu$  and  $\kappa$  based on *ab initio* potential,<sup>36,37</sup> we verify that for low-density gases near ambient temperatures,  $Pr$  is 0.25% and 0.06% less than  $2/3$  for helium and argon, respectively. For these monatomic gases  $c_V \approx (3/2)k_B$  and  $Pr \approx 2/3$ ; therefore, Eq. (12) becomes

$$\zeta_T = 1.662 \frac{2-h}{h}. \quad (13)$$

TABLE I. Experimental values of accommodation coefficient  $h$  near 273.16 K, corresponding values of temperature jump coefficient  $\zeta_T$  calculated by Eq. (13), and combinations of  $\alpha_t$  and  $\alpha_n$  providing the same value of  $\zeta_T$  according to Eq. (15).

Gas	Surface	References	$h$	$\zeta_T$	$\alpha_t$	$\alpha_n$
He	ETP-Cu <sup>a</sup>	22 <sup>b</sup>	$0.399 \pm 0.15^c$	$6.67 \pm 0.32^d$	0.7	0.037
	ETP-Cu	21	$0.3926 \pm 0.0010$	$6.805 \pm 0.022$	0.7	0.027
	OFHC-Cu <sup>e</sup>	16	$0.38 \pm 0.01$	$7.1 \pm 0.2$	0.7	0.007
	SS <sup>f</sup>	14	$0.38 \pm 0.05$	$7.1 \pm 1.3$	0.7	0.007
Ar	Al <sup>g</sup>	9	$0.84 \pm 0.05$	$2.30 \pm 0.25$	0.9	0.85
	ETP-Cu	15	$0.80 \pm 0.03$	$2.55 \pm 0.16$	0.9	0.76
	ETP-Cu	17	$0.777 \pm 0.013$	$2.62 \pm 0.07$	0.9	0.74

<sup>a</sup>Electrolytic-tough-pitch copper.

<sup>b</sup>Preliminary results using helium in this resonator are consistent with  $h = 0.40 \pm 0.02$  in the range of 235–362 K (Ref. 38).

<sup>c</sup>The uncertainties for  $h$  are those provided by the original authors and correspond to one standard uncertainty.

<sup>d</sup>The uncertainties for the temperature jump coefficient are propagated from the uncertainty of  $h$ .

<sup>e</sup>Oxygen-free-high-conductivity copper.

<sup>f</sup>Stainless steel.

<sup>g</sup>Aluminum alloy.

From this expression, we conclude that the minimum value of the temperature jump coefficient calculated from the elementary kinetic theory<sup>35</sup> is 1.662 when  $h = 1$ . However, the jump coefficient  $\zeta_T$  calculated from the kinetic Boltzmann equation assuming  $h = 1$  is significantly larger and equal to

$$\zeta_T = 1.954, \quad (14)$$

according to the review.<sup>7</sup> Thus, the approach to obtain Eq. (12) based on the elementary kinetic theory leads to a significantly smaller value of the temperature jump coefficient in comparison to that obtained from the Boltzmann equation, Eq. (14), even when the same boundary conditions are applied.

In Table I, we list the most precise values of  $h$  determined by acoustic resonator experiments and analyzed by their authors using the expressions (9) and (10). As mentioned above, the relationship between the temperature jump and the ACs depends on the model of the gas surface interaction. To avoid this dependence, we recommend reporting experimental results in terms of the temperature jump coefficient  $\zeta_T$  using Eq. (4). The fifth column of Table I contains the values of the jump coefficient  $\zeta_T$  that we extracted from the experimental data<sup>9,10,15–17,21,22</sup> using the relation (13).

The second column in Table I identifies the metals surrounding the gas-filled cavities. Within the resolution of the measurements, the values of  $\zeta_T$  are independent of which metal comprises the walls of the cavities; however,  $\zeta_T$  for helium and argon differ significantly from each other. We have no certain explanation for this remarkable independence of the wall metal. We note that the resonators were not baked out under high vacuum conditions; instead, they were exposed for many days to flows of highly purified gases. We speculate that the metal surfaces were covered with oil or water layers, perhaps only a few molecules thick, that hid the differences between the metal substrates. The oil comprising such a layer may originate in vacuum pumps.

Besides the rigorous kinetic equation describing the intermolecular collisions, a reliable model of the gas–surface interaction should be applied. The widely used diffuse-specular model contains only one parameter and does not allow the description of a wide range of experiments. That is why the CL model is more suitable for our purpose and will be used below. The numerical values of the jump coefficient  $\zeta_T$  for various values of  $\alpha_t$  and  $\alpha_n$  were reported in Refs. 5 and 34. In contrast to the common opinion that the temperature jump coefficient is determined only by the NEAC and independent of the TMAC, it was shown that the jump coefficient is sensitive to both ACs  $\alpha_t$  and  $\alpha_n$ .<sup>5,34</sup> Thus, if both  $\alpha_t$  and  $\alpha_n$  are known, then the jump coefficient can be calculated applying the methodology described in Refs. 5 and 34.

## IV. EXPERIMENTAL VALUES OF ACCOMMODATION COEFFICIENTS

### A. Resonators

In this section, we combine the resonator values of the temperature jump coefficient  $\zeta_T$  with flow-derived values of  $\alpha_t$  to estimate TMAC and NEAC for machined metal

surfaces. To do this, we assume that metal surfaces of the resonators and of the flow apparatus are equivalent.

To determine the constraints on TMAC and NEAC from the experimental values of  $\zeta_T$  listed in Table I, we need a relation of  $\zeta_T$  to  $\alpha_t$  and  $\alpha_n$  obtained from numerical solution of the Boltzmann kinetic equation subject to the CL boundary condition. A method to solve such a problem based on Shakhov's model<sup>3,39</sup> is described in details previously<sup>5</sup> and omitted here. Following the method, we calculated the jump coefficient  $\zeta_T$  with a numerical error below 0.1% for several values of the ACs  $\alpha_t$  and  $\alpha_n$  in the ranges  $0 \leq \alpha_n \leq 1$  and  $0.6 \leq \alpha_t \leq 1$  with the step 0.1. These ranges span all possible in practice values of  $\alpha_t$  and  $\alpha_n$  for any gas. A convenient representation of the numerical results for  $\zeta_T(\alpha_n, \alpha_t)$  within the tolerance of 0.1% is given by the following interpolating formula:

$$\zeta_T = \frac{95.68 - 35.23\alpha_n + 3.55\alpha_n^2 - 25.27\alpha_t + 12.82\alpha_t^2}{1 + 13.4\alpha_n + 23.96\alpha_t - 11.97\alpha_t^2}, \quad (15)$$

which was obtained using the commercial software package TABLECURVE 3D, version 4.0.<sup>40</sup> In the diffuse scattering limit,  $\alpha_t = 1$  and  $\alpha_n = 1$ , Eq. (15) provides the value given by Eq. (14).

According to this relation, not only one pair of ACs provides some specific value of the jump coefficient  $\zeta_T$ , but a continuous set of values of  $\alpha_t$  and  $\alpha_n$  leads to the same jump coefficient. Figure 1 displays shaded regions that are consistent with the temperature jump data from resonators listed in Table I. For the helium, the shaded region denoted "He resonance" spans the range  $6.35 \leq \zeta_T \leq 7.0$ ; for argon, the shaded region "Ar resonance" spans the range  $2.05 \leq \zeta_T \leq 2.7$ . Using additional information about the TMAC, we can reduce the regions of ACs corresponding the experimental values of the jump coefficient given in Table I.

The TMAC has been measured previously by many other methods different from the acoustic resonance. Its values extracted from experimental data on the velocity slip

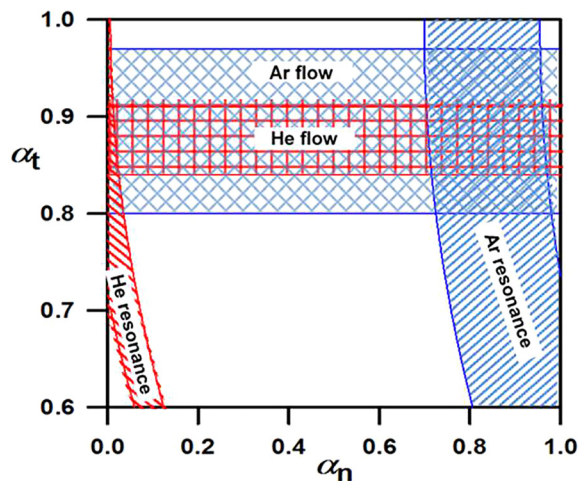


FIG. 1. (Color online) Shaded areas are values of  $\alpha_t$  and  $\alpha_n$  consistent with resonance data from Table I and with flow data (Refs. 6 and 7).

coefficient are given in Table 6 of Ref. 7. Some values extracted from measurements of mass flow rate of gases through long pipes are reported in Ref. 6. Summarizing these data, it can be said that for smooth solid surfaces the TMAC  $\alpha_t$  varies in the ranges  $0.84 \leq \alpha_t \leq 0.91$  for helium and  $0.80 \leq \alpha_t \leq 0.97$  for argon. If a surface is atomically clean, the TMAC for helium can be as small as 0.71.<sup>41</sup> Figure 1 displays the values of TMAC from the papers<sup>6,7</sup> as horizontal bands named as "Ar flow" and "He flow." If the surfaces of the resonators are comparable to the surfaces of the flow channels, the intersection of the domains "He flow" and "He resonance" in Fig. 1 puts tight constraints on the values of  $\alpha_t$  and  $\alpha_n$  at ambient temperature for helium. The intersection of "Ar flow" and "Ar resonance" in Fig. 1 indicates the set of possible ACs for argon. Some pairs of  $\alpha_t$  and  $\alpha_n$  from these sets related to the experimental values of the jump coefficient  $\zeta_T$  by Eq. (15) are given in the sixth and seventh columns of Table I.

## B. Heat transfer between coaxial cylinders

Previously, the NEAC was estimated<sup>27</sup> using experimental data on heat transfer between two coaxial cylinders.<sup>25</sup> The estimation points out that the NEAC  $\alpha_n$  is not larger than 0.1 for helium and it is close to unity for argon. Here, a more detailed analysis of these experimental data is done, i.e., the heat flux is calculated for more pairs of the ACs and hence more accurate values of the NEAC are extracted. For this purpose, the dimensionless heat flux defined as

$$\tilde{q} = \frac{q}{pv_m \Delta T} \quad (16)$$

will be used. Here,  $q$  is actual heat flux,  $p$  is the gas pressure,  $T$  is its average temperature, and  $\Delta T$  is the temperature difference between the cylinders.

The experimental data for helium<sup>25</sup> are given in the range of the rarefaction parameter  $\delta$  from 0.009 to 0.18, which practically represents the free-molecular regime. To extract the ACs from these data, the dimensionless heat flux  $\tilde{q}$  was calculated by the method described in Ref. 27 for four combinations of the ACs ( $\alpha_t, \alpha_n$ ): (0.9, 0.0), (0.9, 0.1), (0.7, 0.0), and (0.7, 0.1). A comparison of the experimental data<sup>25</sup> with the numerical values of  $\tilde{q}$  presented in Fig. 2 shows a good agreement between the theory and experiment for the combinations (0.9, 0.0) and (0.7, 0.1). Thus, we conclude that the NEAC  $\alpha_n$  is certainly smaller than 0.1, which is consistent with its values extracted from the acoustic resonator data given in Table I. If we assume that the ACs for helium varies in the ranges  $0.7 \leq \alpha_t \leq 0.9$  and  $0 < \alpha_n \leq 0.1$ , the jump coefficient  $\zeta_T$  will vary from 5.6 to 7.1 according to Eq. (15).

The experimental values of the heat flux through argon<sup>25</sup> span the rarefaction parameter  $\delta$  range from 0.06 to 4. The data for larger values of  $\delta$  have smaller uncertainty since the heat flux is larger in this regime. A comparison of these data with Eq. (7) allows us to extract the temperature jump coefficient. Combining Eqs. (7) and (16), the dimensionless heat flux in the temperature jump regime is obtained as

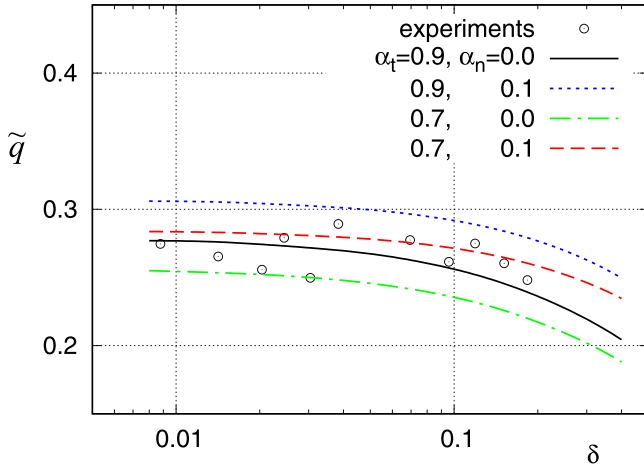


FIG. 2. (Color online) Experimental data (Ref. 25) (symbols) of heat flux through helium between two coaxial cylinders and its numerical values (curves) based on the theory (Ref. 27).

$$\tilde{q} = \frac{15}{8\delta} \left[ \ln \frac{b}{a} + \frac{\zeta_T}{\delta} \left( 1 + \frac{a}{b} \right) \right]^{-1} \quad \text{at } r = a, \quad (17)$$

where the value  $Pr = 2/3$  has been used. The curves corresponding to three values of the jump coefficient  $\zeta_T = 1.954, 3$  and  $5$  are plotted in Fig. 3 along with the experimental values of the heat flux.<sup>25</sup> Note that, the first value corresponds to the diffuse scattering, Eq. (14), and it is the lowest among all the other values. The comparison shows that the best agreement between the theory and experiment is reached at  $\zeta_T = 3$ . The most realistic combination of ACs corresponding to this value of the jump coefficient is  $\alpha_t = 0.92$  and  $\alpha_n = 0.61$ . The value  $0.92$  of  $\alpha_t$  was extracted from the Poiseuille flow; see Table 6 of Ref. 7. The value  $0.61$  of  $\alpha_n$  obtained using Eq. (15) is 20% smaller than the average value  $\alpha_n = 0.78$  extracted from the acoustic resonator experiments and given in Table I. Considering that the jump coefficient extracted from any kind of experiment has a relatively large uncertainty, the discrepancy of 20% for two

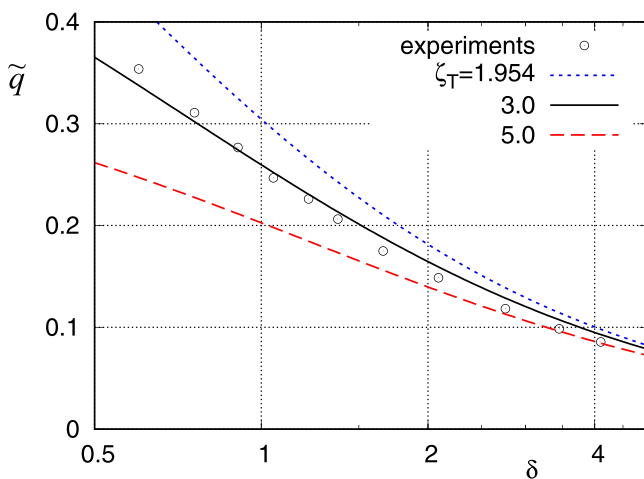


FIG. 3. (Color online) Experimental data (symbols) reported in Ref. 25 of heat flux through argon between two coaxial cylinders and analytical solution (curves) based on Eq. (7).

completely different experiments can be considered reasonable. The conclusion about the variation in the range of the temperature jump coefficient of argon can be made from the data given in Table I and the value extracted from the experiments,<sup>25</sup> that is,  $2.3 \leq \zeta_T \leq 3.0$ . This range of  $\zeta_T$  corresponds to the ACs variation in the ranges  $0.8 \leq \alpha_t \leq 0.9$  and  $0.61 \leq \alpha_n \leq 0.85$ .

Thus, the values of the NEAC  $\alpha_n$  for both helium and argon extracted from the experimental results on cylindrical heat transfer<sup>25</sup> are consistent with those based on the acoustic resonance experiments and given in Table I.

### C. Heat transfer between two planar plates

Experimental results on heat transfer between two parallel planar plates made from various kinds of materials were reported in Ref. 26, where the diffuse-specular model was used to extract the AC. The measurements were carried out in a wide range of the gas rarefaction parameter. Since the influence of the gas–surface interactions on the heat flux is maximum in the free-molecular limit ( $\delta \rightarrow 0$ ), it is reasonable to use the data in this limit to extract the TMAC and NEAC. Trott *et al.*<sup>26</sup> did not report the heat flux values; instead, they presented their results in terms of the AC  $h$ . In the free-molecular limit, the heat flux between two plates under the diffuse-specular scattering reads

$$\tilde{q} = \frac{1}{\sqrt{\pi}} \frac{h}{2-h} \quad \text{at } \delta \rightarrow 0, \quad (18)$$

where  $\tilde{q}$  is defined by Eq. (16). If we replace the diffuse-specular scattering by the CL model, then the same quantity takes the form

$$\tilde{q} = \frac{1}{2\sqrt{\pi}} \left[ \frac{\alpha_n}{2-\alpha_n} + \frac{\alpha_t(2-\alpha_t)}{2-\alpha_t(2-\alpha_t)} \right] \quad \text{at } \delta \rightarrow 0, \quad (19)$$

where Eqs. (2) and (16) have been combined.

Table II shows values of  $h$  reported in Ref. 26, the corresponding dimensionless heat flux  $\tilde{q}$  calculated by Eq. (18) and possible pairs of  $\alpha_t$  and  $\alpha_n$  providing the same value of the heat flux when calculated by Eq. (19). Again, these data show that the NEAC for helium is very small, i.e.,  $\alpha_n = 0.01$ , while for argon it is close to unity, i.e.,  $0.84 \leq \alpha_n \leq 0.93$ . These results also suggest that a treatment of metal surfaces by plasma reduces both the TMAC and NEAC.

### V. DISCUSSION AND CONCLUSIONS

Recently, measurements of the acoustic resonance frequencies  $f_{\text{acoustic}}$  of the longitudinal modes of argon-filled cylindrical cavities have been used to determine the Boltzmann constant  $k_B$  (Ref. 18) and they will be used to determine the thermodynamic temperature  $T$ , particularly at its high values.<sup>19,23</sup> For the lowest possible uncertainties, these measurements must consider the effects of both the temperature jump and the velocity slip at the gas–solid interface. Suppose the cylinder's axis is coincident with the  $z$ -coordinate axis and one end of the cylinder is located at  $z = 0$ . For the longitudinal modes, the acoustic velocity has

TABLE II. Experimental values (Ref. 26) of accommodation coefficient  $h$ , dimensionless heat flux calculated by Eq. (18), and ACs extracted by Eq. (19).

Gas	Surface	$h$	$\tilde{q}$	$\alpha_t$	$\alpha_n$
He	SS <sup>a</sup>	$0.46 \pm 0.02^b$	$0.168 \pm 0.010^c$	0.49	0.01
	Al <sup>d</sup>	$0.47 \pm 0.02$	$0.173 \pm 0.010$	0.51	0.01
	Pl <sup>e</sup>	$0.58 \pm 0.02$	$0.230 \pm 0.011$	0.68	0.01
	SS-pl <sup>f</sup>	$0.38 \pm 0.02$	$0.132 \pm 0.009$	0.40	0.01
	Al-pl <sup>g</sup>	$0.38 \pm 0.02$	$0.132 \pm 0.009$	0.40	0.01
	Pl-pl <sup>h</sup>	$0.52 \pm 0.02$	$0.198 \pm 0.010$	0.58	0.01
Ar	SS	$0.95 \pm 0.02$	$0.510 \pm 0.021$	0.95	0.92
	Al	$0.96 \pm 0.02$	$0.521 \pm 0.021$	1.0	0.93
	Pl	$0.96 \pm 0.02$	$0.521 \pm 0.021$	1.0	0.93
	SS-pl	$0.90 \pm 0.02$	$0.462 \pm 0.019$	0.9	0.84
	Al-pl	$0.91 \pm 0.02$	$0.471 \pm 0.019$	0.9	0.85
	Pl-pl	$0.94 \pm 0.02$	$0.500 \pm 0.020$	0.95	0.90

<sup>a</sup>Machined stainless steel.

<sup>b</sup>Uncertainty declared in Ref. 26 and based only on repeatability in measurements.

<sup>c</sup>Uncertainties propagated from the uncertainty of  $h$ .

<sup>d</sup>Machined aluminum.

<sup>e</sup>Machined platinum.

<sup>f</sup>Machined stainless steel treated by plasma.

<sup>g</sup>Machined aluminum treated by plasma.

<sup>h</sup>Machined platinum treated by plasma.

only a  $z$ -component  $v_z \propto \sin(z)$ . Furthermore,  $v_z$  is independent of the  $x$ - and  $y$ -coordinates, except near the solid, stationary wall that bounds the cavity. At the gas-wall boundary, momentum and heat are exchanged between the oscillating gas and the wall during each acoustic cycle. In response to the momentum exchange, a viscous boundary layer extends from the wall into the cylinder. In this layer,  $v_z$  grows from zero at the wall (ignoring slip) to  $v_z$  with the characteristic length  $\delta_v = [\mu/(\pi\varrho f_{\text{acoustic}})]^{1/2}$ , where  $\varrho$  is the mass density of the gas. According to Moldover *et al.*,<sup>20</sup> the boundary layer adds a measurable term to  $f_{\text{acoustic}}$  that varies as  $-p^{1/2}$  at low gas pressures because under such conditions  $p \propto \varrho$ .

In principle, measurements of  $f_{\text{acoustic}}$  of several modes of a cylindrical cavity can be analyzed to determine values of  $\alpha_t$  and  $\alpha_n$ . In practice, the resulting uncertainties of  $\alpha_t$  and  $\alpha_n$  will be larger than those in Table I because the acoustic modes of a cylindrical cavity have lower signal-to-noise ratios for measuring  $f_{\text{acoustic}}$  than the modes of quasispherical cavities of equal volume. Even with large uncertainties, resonator-derived values of  $\alpha_t$  would be of interest to better understand gas–surface interactions. For the most accurate measurements of thermodynamic temperatures, it may be useful to conduct slip-sensitive flow measurements to determine  $\alpha_t$  for argon–solid interfaces similar to those used in high-temperature resonators.

We pointed out that presentations of experimental results for gas–surface interactions in terms of ACs are model-dependent and should be avoided. Therefore, we recommend that future presentations of resonator results use the well-defined temperature jump coefficient. In addition, future results on a heat flux between two surfaces will be more

valuable when experimental values of the heat flux itself are presented instead of data on extracted ACs. We note that a derivation of ACs from any kind of experimental data is not trivial task requiring a numerical calculation of the kinetic equation together with a reliable model of the gas–surface interaction.

We reviewed the temperature jump coefficients determined by experimental data from spherical acoustic resonators. First, this coefficient has been calculated applying the CL model of the gas–surface interactions for the whole range of the NEAC, while only those values of the TMAC that are usually observed in practice have been considered. These data have been used to extract the NEAC from the experimental values of the temperature jump coefficient for helium and argon. To check the consistency of these data, the same coefficients were extracted from experimental data on heat transfer between two coaxial cylinders and two parallel plates. Analyzing all these data, it was found that the NEAC of helium varies in the range  $0 < \alpha_n \leq 0.1$ . The same coefficient for argon varies in the range  $0.61 \leq \alpha_n \leq 0.93$ . The variations of the temperature jump coefficient are  $5.6 \leq \zeta_T \leq 7.1$  and  $2.3 \leq \zeta_T \leq 3.0$  for helium and argon, respectively. These values span all most types of smooth metallic surfaces.

Since the temperature jump coefficient is sensitive to both the TMAC and NEAC, their values can be extracted more precisely from different types of experiments made with the same surface and gas. For instance, two rotating disks can be used to measure the shear stress and subsequently to calculate the TMAC. The same disks having different temperatures can be employed to measure the heat flux between them, which can then be used to calculate the NEAC. Similar experiments can be performed with two coaxial cylinders.

## ACKNOWLEDGMENT

F.Sh. is thankful to CAPES (Brazil) for the support of his long term visit to NIST (Grant BEX 0306/15-0).

- 1J. H. Ferziger and H. G. Kaper, *Mathematical Theory of Transport Processes in Gases* (North-Holland, Amsterdam, 1972).
- 2C. Cercignani, *The Boltzmann Equation and Its Application* (Springer-Verlag, New York, 1988).
- 3F. Sharipov, *Rarefied Gas Dynamics. Fundamentals for Research and Practice* (Wiley-VCH, Berlin, 2016).
- 4C. Cercignani and M. Lampis, *Transp. Theory Stat. Phys.* **1**, 101 (1971).
- 5F. Sharipov, *Eur. J. Mech. B/Fluids* **22**, 133 (2003).
- 6F. Sharipov, *Eur. J. Mech. B/Fluids* **22**, 145 (2003).
- 7F. Sharipov, *J. Phys. Chem. Ref. Data* **40**, 023101 (2011).
- 8J. Mehl and M. Moldover, *J. Chem. Phys.* **74**, 4062 (1981).
- 9M. B. Ewing, M. L. McGlashan, and J. P. M. Trusler, *Metrologia* **22**, 93 (1986).
- 10M. R. Moldover, J. P. M. Trusler, T. J. Edwards, J. B. Mehl, and R. S. Davis, *J. Res. Natl. Bur. Stand.* **93**, 85 (1988).
- 11J. Mehl, M. Moldover, and L. Pitre, *Metrologia* **41**, 295 (2004).
- 12L. Pitre, M. Moldover, and W. Tew, *Metrologia* **43**, 142 (2006).
- 13M. Moldover, *C. R. Phys.* **10**, 815 (2009).
- 14R. M. Gavioso, G. Benedetto, P. A. G. Albo, D. M. Ripa, A. Merlone, C. Guianvarc'h, F. Moro, and R. Cuccaro, *Metrologia* **47**, 387 (2010).
- 15L. Pitre, F. Sparasci, D. Truong, A. Guillou, L. Risehari, and M. E. Himbert, *Int. J. Thermophys.* **32**, 1825 (2011).
- 16R. M. Gavioso *et al.*, *Int. J. Thermophys.* **32**, 1339 (2011).

- <sup>17</sup>M. de Podesta, R. Underwood, G. Sutton, P. Morantz, P. Harris, D. F. Mark, F. M. Stuart, G. Vargha, and G. Machin, *Metrologia* **50**, 354 (2013).
- <sup>18</sup>H. Lin, X. J. Feng, K. A. Gillis, M. R. Moldover, J. T. Zhang, J. P. Sun, and Y. Y. Duan, *Metrologia* **50**, 417 (2013).
- <sup>19</sup>X. Feng, K. A. Gillis, M. R. Moldover, and J. B. Mehl, *Metrologia* **50**, 219 (2013).
- <sup>20</sup>M. R. Moldover, R. M. Gavioso, J. B. Mehl, L. Pitre, M. de Podesta, and J. T. Zhang, *Metrologia* **51**, R1 (2014).
- <sup>21</sup>L. Pitre, L. Risegari, F. Sparasci, M. D. Plimmer, M. E. Himbert, and P. A. G. Albo, *Metrologia* **52**, S263 (2015).
- <sup>22</sup>R. M. Gavioso, D. M. Ripa, P. P. M. Steur, C. Gaiser, D. Truong, C. Guianvarc'h, P. Tarizzo, F. M. Stuart, and R. Dematteis, *Metrologia* **52**, S274 (2015).
- <sup>23</sup>K. Zhang, X. J. Feng, K. Gillis, M. Moldover, J. T. Zhang, H. Lin, J. F. Qu, and Y. N. Duan, *Philos. Trans. R. Soc. A* **374**, 20150049 (2016).
- <sup>24</sup>R. Underwood, M. de Podesta, G. Sutton, L. Stanger, R. Rusby, P. Harris, P. Morantz, and G. Machin, *Philos. Trans. R. Soc. A* **374**, 20150048 (2016).
- <sup>25</sup>Y. G. Semyonov, S. F. Borisov, and P. E. Suetin, *Int. J. Heat Mass Transfer* **27**, 1789 (1984).
- <sup>26</sup>W. M. Trott, J. N. Castaneda, J. R. Torczynski, M. A. Gallis, and D. J. Rader, *Rev. Sci. Instrum.* **82**, 035120 (2011).
- <sup>27</sup>F. Sharipov and G. Bertoldo, *J. Vac. Sci. Technol., A* **24**, 2087 (2006).
- <sup>28</sup>T. Edmonds and J. P. Hobson, *J. Vac. Sci. Technol.* **2**, 182 (1965).
- <sup>29</sup>F. Sharipov, *Handbook of Vacuum Technology*, edited by K. Jousten, 2nd ed. (Wiley-VCH, Berlin, 2016), Chap. 5, pp. 167–228.
- <sup>30</sup>F. Sharipov, *Microfluidics and Nanofluidics Handbook: Chemistry, Physics, and Life Science Principles*, edited by S. Mitra and S. Chakraborty (CRC, Boca Raton, FL, 2011).
- <sup>31</sup>Y. Sone, T. Ohwada, and K. Aoki, *Phys. Fluids A* **1**, 363 (1989).
- <sup>32</sup>S. K. Loyalka, *Physica A* **163**, 813 (1990).
- <sup>33</sup>L. B. Barichello and C. E. Siewert, *Eur. J. Appl. Math.* **11**, 353 (2000).
- <sup>34</sup>C. E. Siewert, *Phys. Fluids* **15**, 1696 (2003).
- <sup>35</sup>E. H. Kennard, *Kinetic Theory of Gases* (McGraw-Hill, New York, 1938).
- <sup>36</sup>E. Bich, R. Hellmann, and E. Vogel, *Mol. Phys.* **105**, 3035 (2007).
- <sup>37</sup>E. Vogel, B. Jaeger, R. Hellmann, and E. Bich, *Mol. Phys.* **108**, 3335 (2010).
- <sup>38</sup>R. M. Gavioso, private communication (13 July 2016).
- <sup>39</sup>E. M. Shakhov, *Fluid Dyn.* **3**, 95 (1968).
- <sup>40</sup>In order to describe procedures adequately, it is occasionally necessary to identify commercial products by manufacturers' name. In no instance does such identification imply endorsement by the National Institute of Standards and Technology nor does it imply that the particular product or equipment is necessarily the best available for the purpose.
- <sup>41</sup>O. V. Sazhin, S. F. Borisov, and F. Sharipov, *J. Vac. Sci. Technol., A* **19**, 2499 (2001); **20**, 957 (2002).